MECHANICS OF SINGLE MOLECULES

Lecture Outline

Miklós S.Z. Kellermayer, M.D., Ph.D.

College on Biophysics:
From Genetics to Structural Biology
Trieste, Italy, 2001

The contents of this lecture outline are solely for educational purposes.

Contact information:

Miklós S.Z. Kellermayer, M.D., Ph.D.
Department of Biophysics
University of Pécs, Faculty of Medicine
Szigeti ut 12., H-7624 Pécs, Hungary
Tel: (36-72) 536271; Fax: (36-72) 536261
E-mail: Miklos.Kellermayer.Jr@aok.pte.hu

CONTENTS

INTRODUCTION

The last decade has seen an erupting development in the research of single molecules. The driving force behind single-molecule reseach has been several-fold: instrumental advancements in detector and force-measuring technologies, the desire to understand the mechanism of action of biological machines and to manufacture similar machines of micro- and nanometer dimensions, just to name a few. The goal of the lecture series, held at the Abdus Salam International Centre for Theoretical Physics in Trieste, Italy between October 8-10, 2001, is to provide a glimpse at the fundamentals of single-molecule research with a focus on mechanical aspects. What follows is a detailed outline of three lectures which address various issues of single-molecule research: 1) single-molecule methods, 2) elasticity of single nucleic acid molecules and nucleoprotein complexes, 3) elasticity and unfolding of single protein molecules, and 4) intermolecular interactions at the single-molecule level.

WHY STUDY SINGLE MOLECULES?

Most of our knowledge in biology, chemistry and physics is derived from ensembles of molecules with the inherent assumption that under identical conditions molecules of identical composition behave more or less the same way. Recent findings of single-molecule experiments suggest, however, that molecules of the same species may follow quite different paths during transition from one state to another. Thus, single-molecule methods may provide novel insights into how molecules and molecular systems behave. Single-molecule methods have several advantages over ensemble techniques: 1) spatial and temporal averaging is avoided, 2) temporal synchronisation is not necessary when investigating processes as a function of time, 3) novel phenomena may be discovered, which are otherwise averaged, and therefore remain hidden, in ensembles (e.g., flicker), and 4) anisotropic mechanical effects may be investigated. The methods of exerting such mechanical effects on single molecules and the analysis and interpretation of the derived information are the main focus of the following chapters.

PRINCIPLES AND TECHNIQUES OF SINGLE-MOLECULE MANIPULATION

In order to mechanically manipulate single molecules, one must grab them with suitable handles and measure the tiny forces that are generated. Two main methods have been used to manipulate single molecules: 1) optical and 2) cantilever-based methods. Optical methods utilize the mechanical characteristics of photons, while cantilever-based methods use flexible beams or levers. The optical tweezer and the atomic force microscope are introduced here, as best representatives of the optical and cantilever-based methods, respectively. For selected reviews see [1-7].

A. Optical tweezer

In the optical tweezer (synonyms: optical trap, laser trap, laser tweezer), radiation pressure is utilized for exerting mechanical forces. According to deBroglie's relation, electromagnetic radiation carries momentum, $P=h/\lambda$, where h is Planck's constant and λ is the wavelength of the radiation. A photon flux interacting with an object will, therefore, impose mechanical force, albeit miniscule, on that object. The interaction between photons and the object may take several forms, including reflection, refraction, diffraction and absorption. In the optical tweezer, reflection and refraction are the most important. As a light beam interacts with an object, say a refractive microscopic bead (**Figure 1.a**), its direction, hence momentum changes. By the law of conservation of momentum, the momentum of the bead, too, changes equally but in opposite direction. According to the Second Law of Newton, the rate of momentum change produces mechanical force; therefore, the bead will be mobilized in the direction of its momentum change (**Figure 1.a**). In the optical tweezer the bead interacts not with a hypothetical, infinitely narrow light beam as in **Figure 1.a**, but experiences the counteracting optical forces that arise in a gradient electromagnetic field (**Figure 1.b**). In equilibrium, the counteracting optical forces, most notably the *gradient* and *scattering* forces, acting on the bead are equal and therefore cancel out. For a given optical power the scattering force, which acts in the direction of beam propagation, is proportional to the illuminated area of bead surface, while the gradient force, which acts in the direction of the light

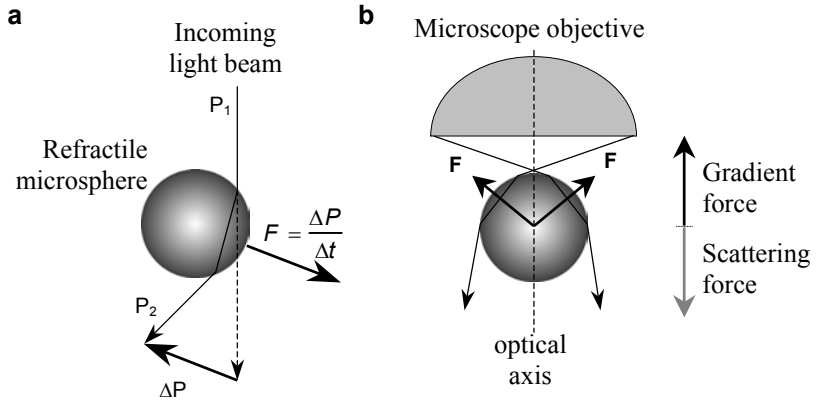

Figure 1. Principles of the optical tweezer. **(a)** Interaction between a light beam and a refractile microsphere, indicating the change in the momentum (P) of both. **(b)** Microsphere captured in the laser trap, showing the equilibrium of the gradient and scattering optical forces.

intensity change, is proportional to the field gradient. Large field gradients, which correspond to the change in spatial light intensity distribution, typically appear when an intense light beam, for example, a laser beam, is brought to a diffraction-limited focus by an optical lens such as the microscope objective. To displace a bead from its equilibrium position in the center of the optical trap, external mechanical force is required. Conversely, the displacement of the bead from the trap center reflects the effect of external force, whose magnitude, within limits, is linearly proportional to the magnitude of bead displacement. Thus, the laser tweezer can be utilized as a force transducer (in the piconewton range).

B. Atomic force microscopy

The atomic force microscope (AFM) is a high-resolution scanning probe device in which a sharp cantilever tip is scanned across a surface. The atoms at the tip surface and sample surface interact in an attractive or repulsive manner which deflects the cantilever. The miniscule motions of the cantilever are detected by directing a laser beam on the cantilever which is reflected and projected onto a position-sensing photodiode (**Figure 2.a**). By monitoring the position of the laser beam, sub-angstrom cantilever deflections can be detected, and a surface topographical image is reconstructed. For manipulating single molecules, a modified version of the AFM is used. Such device is often called molecular force probe (MFP). The MFP differs from the AFM (**Figure 2.b**). While the cantilever is scanned across the sample surface in the AFM, it is moved only in vertical direction in the MFP. The MFP is specialized for stretching molecules and measuring their force response. High-resolution vertical cantilever movement in the MFP is achieved by using piezoelectric actuators. The position of the cantilever is directly monitored with either a capacitor or an LVDT (linear voltage differential transformer). As a result, high-resolution force vs. extension curves of single molecules can be measured by using the MFP.

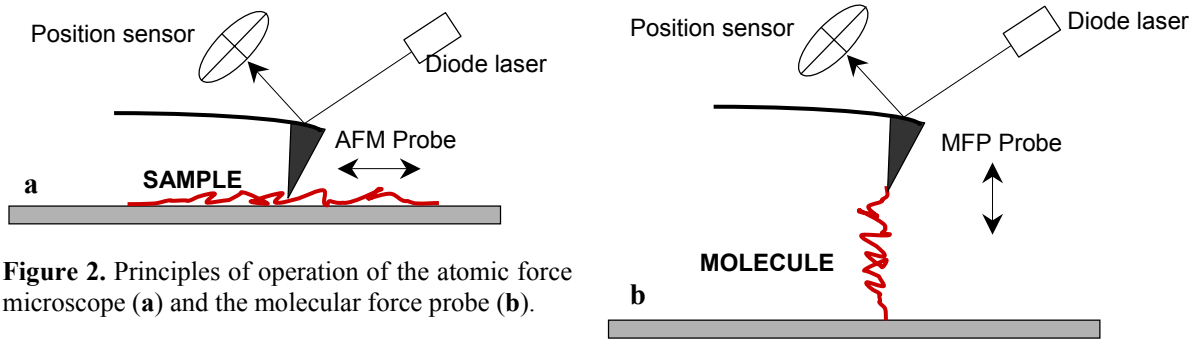

Figure 2. Principles of operation of the atomic force microscope (**a**) and the molecular force probe (**b**).

C. Force measurement and probe stiffness calibration

Optical tweezers and the atomic force microscope work as tensiometers that measure tiny forces in the piconewton range. In order to obtain the forces either the stiffness of the probe must be known or a direct force measurement must be carried out. Stiffness calibration procedures rely on either imposing known forces on the probe or

measuring its thermal fluctuations. The direct force measurement utilizes the principle of conservation of momentum.

1. Stiffness calibration with hydrodynamic drag. Known forces may be imposed on a microscopic bead trapped in the optical tweezer in the form of hydrodynamic drag forces, based on Stokes' law (**Figure 3**). In such a calibration scheme a fluid flow of preadjusted rate (v) is generated, and the corresponding bead displacement is measured. The displacement of the bead from its equilibrium position from the trap center is linearly proportional to the magnitude of the external force within a certain range. Bead displacement may be quantitated by following either the position of the bead image or the laser beam leaving the trap by using position sensing devices (quadrant photodetector, for example). The flow rate can be established by measuring the velocity of the bead (by using video techniques) as it leaves the trap.

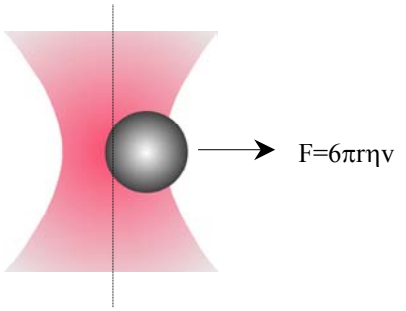

Figure 3. Calibration of the optical tweezer with hydrodynamic drag forces based on Stokes' law.

2. Thermal calibration of probe stiffness. Forces are constantly applied to the probe in the form of thermal agitation. The equipartition theorem may be used to calibrate the probe (either the optical trap or the AFM cantilever) by using this "thermal method." The stiffness of an AFM cantilever in one dimension (in the direction of molecule-pulling) is obtained with the following theoretical considerations. Compliance is

$$C = \frac{|x|}{|F|}, \tag{1}$$

where F is the magnitude of applied force, and x is the magnitude of resulting amplitude of displacement. The inverse of compliance is stiffness (K). Application of simple harmonic force results in oscillation of the body (with mass m). The steady-state movement of the oscillating body is described by

$$x = x_0 \sin(\omega t), \tag{2}$$

where $x_0 = -\frac{F}{m\omega^2}$. Thus, compliance is

$$C = \frac{|x_0|}{|F_0|} = \frac{1}{m\omega^2}. \tag{3}$$

Accordingly, stiffness is $K = m\omega^2$. At resonance, $\omega=\omega_0$ and $K = m\omega_0^2$. Such a simple harmonic oscillator system (mass on a spring, for example) has a total energy (sum of kinetic and potential) of

$$E = \frac{1}{2}mv^2 + \frac{1}{2}Kx^2, \tag{4}$$

where v is velocity. The Hamiltonian of the system is

$$H = \frac{p^2}{2m} + \frac{1}{2} m \omega_0^{\,2} x^2, \tag{5}$$

where p is the momentum of the oscillator. According to the equipartition theorem, each term of the Hamiltonian (i.e., potential and kinetic components) is given by $k_BT/2$, where k_B is Boltzmann's constant, and T is absolute temperature. Of interest to us is the potential energy component, for which

$$\left\langle \frac{1}{2} m \omega_0^{\,2} x^2 \right\rangle = \frac{1}{2} k_B T. \tag{6}$$

The relationship implies that the average potential energy is equivalent to the thermal energy. Since $K = m\omega_0^{\,2}$, therefore

$$\frac{1}{2} K \left\langle x^2 \right\rangle = \frac{1}{2} k_B T. \tag{7}$$

Thus, stiffness can be obtained as

$$K = \frac{k_B T}{\left\langle x^2 \right\rangle}, \tag{8}$$

where $\langle x^2 \rangle$ is the mean square displacement of the cantilever. Thus, if we obtain the mean square displacement of a thermally driven cantilever, the cantilever's stiffness can be calculated. The thermally driven displacement of the cantilever is obtained by sampling the thermal motion of the cantilever at high frequency for a period of time, and analyzing the thermal power spectral density (PSD) function, which is the Fourier transform of the obtained data (vibration amplitude as a function of vibration frequency) (**Figure 4**). Resonance peaks in the PSD correspond to fundamental vibration modes. Typically the lowest mode is analyzed. The height of the resonance peak reflects deviation from ideal rigid body behavior, and can be expressed as the "maximum amplification at resonance" or quality factor (Q). Since the integral of the power spectrum is equivalent to mean square fluctuation in the temporal domain, the cantilever stiffness can be estimated as $K = \frac{k_B T}{P}$, where P is the area of the power spectrum of the thermal fluctuations.

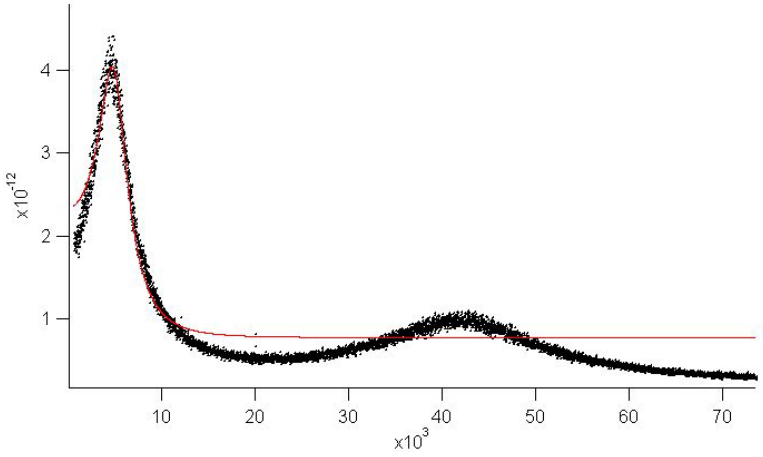

Figure 4. Power spectral density function of the thermal fluctuations of an AFM cantilever (vibration amplitude vs. frequency). A simple harmonic oscillator function was fitted on the lowest vibrational mode.

3. Direct force measurement. The force acting on a bead trapped in the optical tweezer may be directly obtained based on first principles [8]. For a beam of light of power W in a medium of refractive index n, the momentum flux carried by the beam is dP/dt=nW/c, where c is the speed of light. If a particle, such as a bead trapped in the optical tweezer, scatters that light in a new direction, then by conservation of momentum the reaction force on the particle is given by $F=d(P_{in}-P_{out})/dt$ (see also **Figure 1.a**). The force exerted on the particle may be obtained as the integral of radiant intensity across all directions. Thus, if all the photons exiting the trap are collected, then the radiant force exerted on the particle may be directly calculated. The photons exiting the trap are collected with a microscope objective and are projected onto a position-sensing device. In order to collect photons in a relatively wide range of scattering angles, a low incident angle (hence low numerical aperture) optical configuration is used in a dual-beam, counter-propagating arrangement (**Figure 5**) [9, 10].

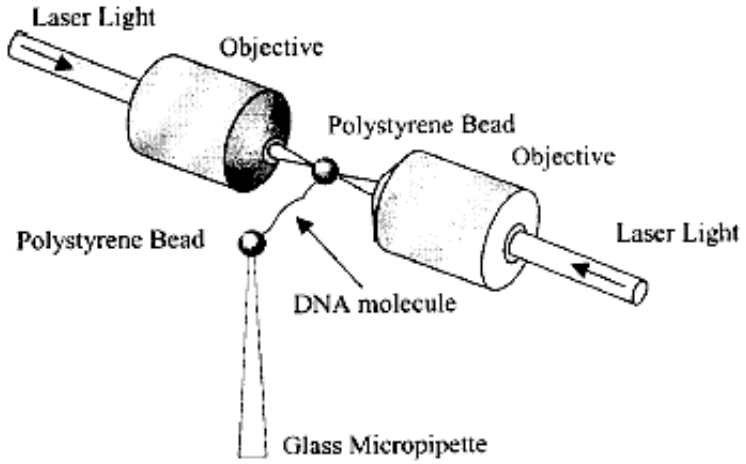

Figure 5. Dual-beam, counter-propagating optical tweezer for direct force measurement.

D. Attachment of molecules

To mechanically manipulate individual biomolecules, their ends have to be mounted with a suitable method. In the optical tweezer, each end of the molecule is attached to different dielectric microscopic beads, the surfaces of which are chemically active and provides reactive sites. The activated microscopic beads serve as "handles" for molecular manipulation. In the AFM, molecules are held between the cantilever tip and a surface, both of which can be chemically activated. Chemically active surfaces carry reactive groups, for example NH_2, COOH, SH. Several different methods have been used to link molecules to the respective surfaces; just to name a few: 1) non-specific adsorption [11], 2) sequence-specific antibodies [12, 13], 3) streptavidin/biotin [8], 4) avidin/biotin, 5) hexahistidine/Ni-NTA, 6) maleimide/SH-group, 7) gold/SH-group [14], 8) photoactivated cross-linkers [12], 9) polyethylene-glycol (PEG) cross-linkers [15].

E. Experimental layout and data analysis.

Once the molecule under investigation is mounted, it is mechanically perturbed either by the action of the investigator or by another molecule (motor protein, e.g.). The typical data recorded are distance (extension, length, displacement) and force. The force data, in case of chain molecules, are typically compared with the predictions of elasticity

models [8, 16]. Deviations from the model usually reflect structural transitions that are subject to further analysis and modelling. In case of motor proteins, the temporal arrangement of the mechanical steps are investigated and the step and stroke sizes are calculated which reflect the processivity and the structural dimensions of the motor molecule [17]. The system-specific force analysis methods are briefly discussed in subsequent chapters. Depending on the techniques used and on the molecular system investigated, different experimental arrangements may be employed. These are briefly introduced below.

1. Stretching a chain with the optical tweezer. **Figure 6** shows a geometric arrangement in which a polymer strand is stretched. In this arrangement different microscopic beads are attached to each end of the molecule. One of the beads is captured in the optical tweezer, and the other one is held by a moveable glass micropipette. The molecule is then

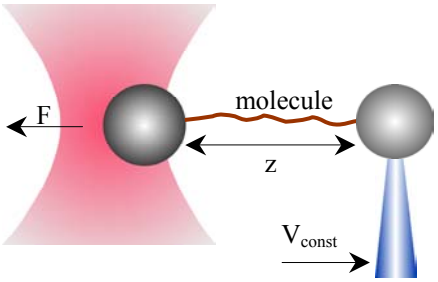

Figure 6. Stretching a single polymer chain by using the optical tweezer. F is the force exerted by the optical trap on the trapped bead, which is equivalent – according to Newton's Third Law – to the force generated in the molecule. z is the end-to-end distance of the chain, and v_{const} is the constant rate at which the molecule is stretched.

stretched by moving the micropipette away from the trap at a constant rate until a user-adjusted, predetermined distance or force is reached. Then, the micropipette is returned towards the trap so that the data corresponding to the release half-cycle may be collected. In this arrangement the length of the molecule is calculated from the distance between the centroids of the beads (obtained by using image processing methods) corrected for the bead radii. The force is obtained from either the change in light momentum or the displacement of the trapped bead from its equilibrium position in the trap center (see above). Other, different geometries have also been used to stretch single polymeric molecules.

2. Studying motor proteins with the optical tweezer. When studying individual motor proteins, the force and the displacement generated by the motor (e.g., myosin) acting on a polymeric molecule (e.g., actin) are measured. Various geometries have been used. In the "three-bead system" (**Figure 7.a**) the motor proteins are attached to a stationary silica bead, and the polymer strand is held between two beads, each of which is captured in an

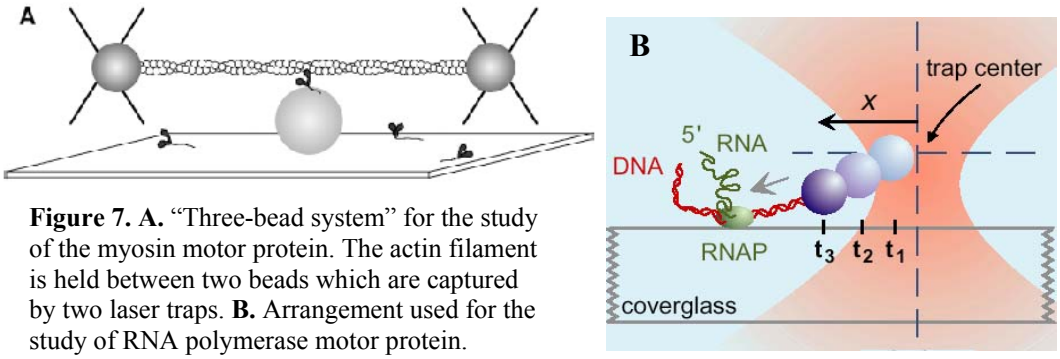

Figure 7. A. "Three-bead system" for the study of the myosin motor protein. The actin filament is held between two beads which are captured by two laser traps. **B.** Arrangement used for the study of RNA polymerase motor protein.

optical trap [18]. In yet another arrangement (**Figure 7.b**) the motor protein may be attached to a substrate (coverglass) and the microsopic bead attached to the end of the polymer strand captured in the trap [19].

3. Stretching molecules with the AFM. Individual polymeric molecules, held between the cantilever tip and a suitable substrate surface, are stretched with the AFM by pulling the cantilever away from the surface (**Figure 8**) [7]. Force is calculated from the bending of the cantilever, and the extension of the molecule is calculated from the cantilever displacement corrected with cantilever bending. Chain-lengthening structural transitions, which arise due to the rupture of intramolecular interactions that staibilize molecular stgructure, are seen as sudden drop in the force trace.

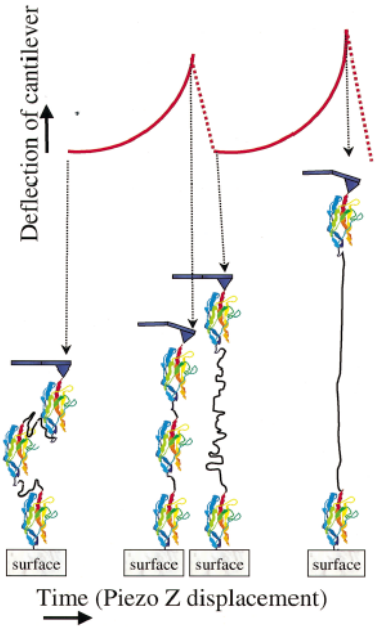

Figure 8. Stretching a molecule (in this case a multi-domain protein) by using the atomic force microscope. The cantilever is moved vertically, away from the surface

4. Studying intermolecular interactions. Interactions between individual molecules (receptor and ligand, e.g.) are studied by placing a load on the intermolecular bond. Either AFM or optical tweezer may be used. **Figure 9** shows an arrangement in which intermolecular interactions are studied with optical tweezer [20].

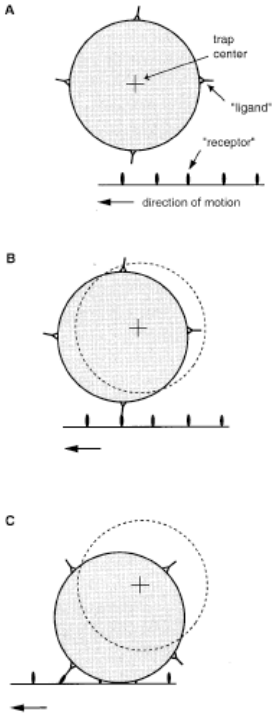

Figure 9. Investigation of intermolecular interactions by using optical tweezer. A receptor-coated suface is displaced relative to a ligand-coated bead captured in the trap. Binding events are manifested in the displacement of the trapped bead from the trap center.

MECHANICS OF NUCLEIC ACID MOLECULES AND NUCLEOPROTEIN COMPLEXES

Deoxyribonucleic acid (DNA), the hereditary material, is tightly packed in the nucleus of every eukaryotic cell. The mechanical properties of DNA, which have been extensively investigated in recent years, are important in understanding its tight packing in the cell nucleus and the structural transitions that occur during its replication and transcription.

A. Elasticity of DNA molecules

Laser tweezer experiments have revealed force-induced structural changes and different elasticity regimes in DNA. Three elasticity regimes may be distinguished [21]:
1. Entropic elasticity. Thermal fluctuations result in the shortening of the DNA strand, resulting in elasticity of entropic nature. For such a, so called, random or entropic chain the end-to-end distance is determined by the thermal energy (k_BT), the contour length, and a statistical length which is conceptually related to the statistical step size in random walk, or the translational diffusion constant in diffusive motion. The statistical segment length describes bending rigidity. The longer the statistical length, the stiffer (more rigid) the chain. Correspondingly, the shorter the statistical length, the greater the force required to extend the chain longitudinally. Two different models have been used to describe the entropic elasticity of DNA. The freely jointed chain (FJC) model considers the chain as a tandem array of orientationally independent, rigid Kuhn segments. The wormlike chain (WLC) model describes the chain as a bendable rod [22], whose bending rigidity is described in terms of persistence length, which is the distance across which the thermally driven bending movements are correlated:

$$\frac{fA}{k_BT} = \frac{z}{L} + \frac{1}{4\left(1-\frac{z}{L}\right)^2} - \frac{1}{4} \qquad (9)$$

where f is force, z and L are the end-to-end and contour lengths of the chain, and A is its persistence length. Although the FJC model can describe DNA entropic elasticity in the

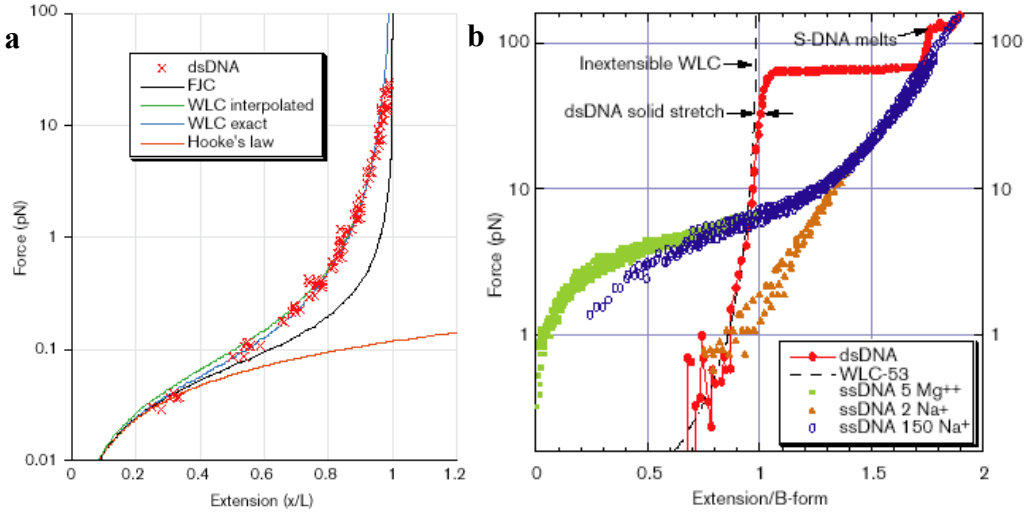

Figure 10. a. Force versus extension curves for λ phage double stranded (ds) DNA pulled in 10 mM Na^+-containing buffer. **b.** Force versus extension curves for λ phage dsDNA and single stranded (ss) DNA.

limit of low forces, the WLC model provides a more precise description at low and intermediate forces (**Figure 10.a**) [21]. For double-stranded DNA in 10 mM Na^+-buffer an excellent fit is obtained with the WLC model using 53 nm as persistence length.

2. Hookean elasticity regime. At the lowest force range the DNA molecule behaves as a Hookean spring for which the extension is directly proportional to force:

$$f = \frac{3k_BT}{2A}\frac{z}{L} \tag{10}$$

For a 10 μm dsDNA molecule a spring constant of approximately 10^{-5} $pNnm^{-1}$ is obtained.

3. Intrinsic elasticity regime. At forces above ~10 pN the end-to-end distance of dsDNA exceeds that predicted by the WLC model, suggesting that the molecule is stretchable and displays a finite stretch modulus. Thus, in this high force regime the elasticity of dsDNA is not purely entropic. The intrinsic elasticity of dsDNA may be described by the following relationship:

$$\frac{z}{L} = 1 - \frac{1}{2}\left(\frac{k_BT}{fA}\right)^{1/2} + \frac{f}{S}, \tag{11}$$

where S is the stretch modulus. S is about 1000 pN for dsDNA in 150 mM Na^+-buffer. The stretch modulus and the intrinsic persistence length (Ai) are related by

$$A_i = \frac{Sr^2}{4k_BT} \tag{12}$$

Assuming a radius of 1 nm for dsDNA, an intrinsic persistence length of 60 nm is obtained, in good agreement with entropic elasticity measurements.

If a dsDNA molecule is subjected to forces above 65 pN, it goes through an apparently cooperative structural change that results in a ~70% increase of contour length of the canonical B-form DNA. The resultant conformation is the so called S-form DNA, which melts into a single strand upon reaching high forces (150-300 pN) (**Figure 10.b**) [21].

B. Chromatin

Chromatin is the complex of DNA with histone proteins, in which nucleosome particles are connected with linker DNA sequences. At forces below 20 pN the chromatin fiber can be described as a stretchable WLC with persistence length of 30 nm and a stretch modulus of 5 pN. A force hysteresis is also observed, suggesting a structural transition between two states (open and closed, see **Figure 11.b**) [9]. At forces above 20 pN, irreversible structural changes occur, which correspond to the dissociation of histones from the DNA strand (**Figure 11.a**) [9].

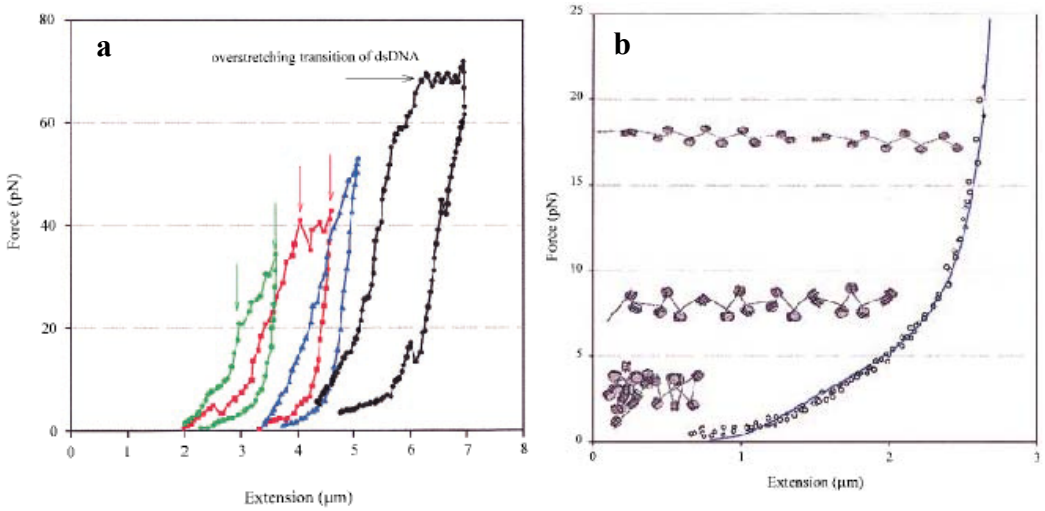

Figure 11. a. Force versus extension curves of repeatedly stretched chicken erythrocyte chromatin fibers from. **b**. Fit of the "release" part of the force versus extension curve of chromatin with an extensible wormlike chain model. The schematics of chromatin structure are indicated on the left.

C. Chromosomes.

Chromosomes are complex supramolecular structures that appear during mitosis (cell division) (**Figure 12.a**) [23]. Chromosomes are formed by the condensation of chromatin. Mitotic chromosomes have recently been measured, with special micropipettes, to be elastic structures. Measurements of the bendig and longitudinal (**Figure 12.b**) elasticities suggest that there are a few rigid axes in the core of the chromosome surrounded by a soft envelope [23]. The rigid core displays elasticity resembling that of titin (see later). Furthermore, during repetitive cycles of stretch-release, chromosomes, just like titin, displayed mechanical fatigue.

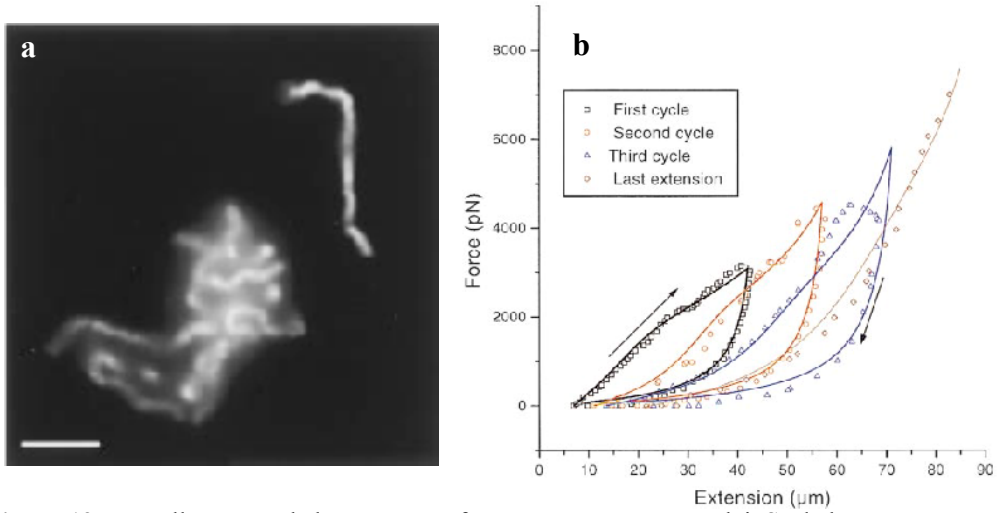

Figure 12. a. Well-separated chromosomes from *Xenopus* sperm nuclei. Scale bar, 5 μm. **b.** Force versus extension cycles of a single chromosome.

D. Elasticity and structure of single RNA molecules

Ribonucleic acids (RNAs) are single-stranded linear polymers of ribonucleotides, and have very important functions in transcribing the genetic code, translating the coded information into protein, and in maintaining the structure of the ribosome. Furthermore, some RNAs have catalytic functions as well. RNAs can fold into three-dimensional structures held together via base-pairing interactions between different, complementary parts along the same chain. The structure and elasticity of sinbgle RNA mlecules may be investigated with single-molecule techniques [24, 25]. Stretching various structural designs of RNA molecules with laser tweezers revealed that these molecules can be unfolded by mechanical force, and when kept in a narrow force range around the critical regime, rapid transition (hopping) occurs between the folded and unfolded states (**Figue 13**) [24].

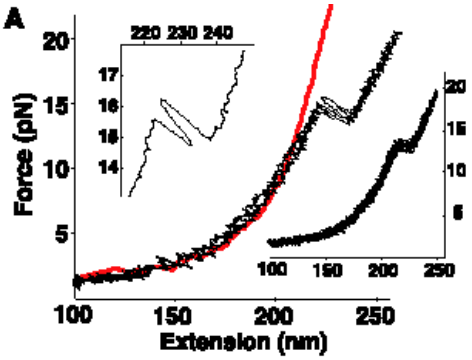

Figure 13. Force vs. extension curves for a single RNA hairpin. Left insert shows the details of hopping.

MECHANICS OF MOTOR PROTEINS

Motor proteins are a ubiquitous family of proteins specialized for the generation of mechanical work (force and displacement) at the expense of chemical energy. Motor proteins are involved in a wide range of cellular functions ranging from the separation of chromosomes during cell division to an ensemble action during muscle contraction An excellent treatise on the subject is [26].

A. Types of motor proteins

Motor proteins can be classified according to the type of polymer they act upon. Accordingly, the following major categories of motor proteins may be identified:

1. Actin-based motor proteins. Actin-based motor proteins belong to the myosin protein family. Currently myosin I-XV classes are distinguished. The two-headed myosin II is also called "conventional myosin," while the rest are called "unconventional myosins." Myosins translocate along F-actin towards the plus or barbed end, but myosin VI has recently been found to travel towards the minus (or pointed) end.

2. Microtubule-based motor proteins. Several motor protein families belong to the microtubule-based motor proteins. These include: *a) Dyneins*, which are either axonemal (ciliary or flagellar) or cytoplasmic dyneins with an average molecular weight of ~500kDa. They translocate along MT towards the minus end. *b) Kinesins*, which are found in neurons and are responsible for vesicle transport along microtubules.The kinesin protein family contains conventional kinesins and isoforms with an average molecular weight of ~110 kDa. Kinesins translocate along microtubules towards the plus end, but there are minus-end-directed proteins as well (e.g., Ncd). c) Dynamins are found in the brain and possess microtubule-dependent GTPase activity. A single polypeptide chain with an average molecular weight of ~100 kDa. Its biological might be vacuolar protein sorting.

3. Nucleic acid-based motor proteins. DNA and RNA polymerases are also motor proteins which translocate along the DNA strand. These are processive motors, which can travel long distances along the polymer strand without dissociation.

B. Common structural and mechanical aspects of motor proteins

1. Structure. N-terminal globular head contains the motor domain that binds and cleaves nucleotide, and carries a specific binding site for the proper cytoskeletal polymer. The C-terminal end contains binding site that determines functionality (e.g., actin-, myosin-, or membrane-binding site).

2. Principle of operation. The principle of motor protein function is cyclic operation. The cycle contains the following major steps: binding to polymer, pulling stroke, dissociation, relaxation. In the meantime, one molecule ATP is hydrolized. Various motor protein-nucleotide kinetic intermediates appear during the cycle. The cycle involves conformational changes of the motor protein. During the mechanical cycle either translocation (isotonic conditions) or force generation (isometric conditions) occur.

3. The duty cycle. The mechanochemistry of motor proteins can be described by their duty cycle. The duty cycle is one period of nucleotide hydrolysis accompanied with the mechanical events (**Figure 14**) [27]. Several simple variables of the cycle may be identified.

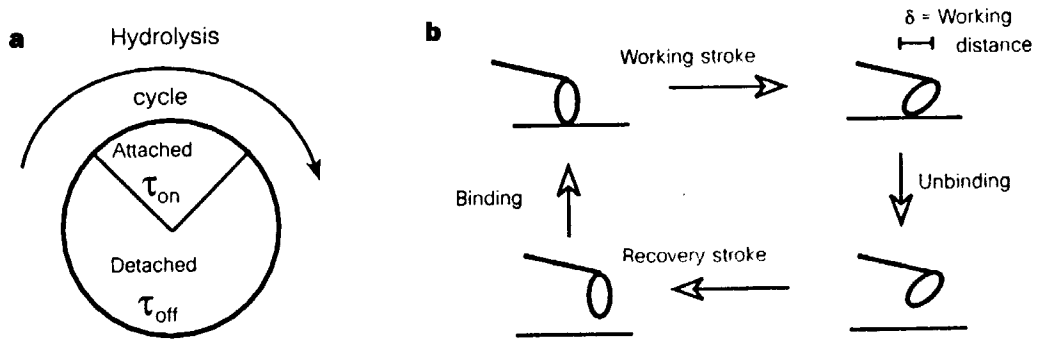

Figure 14. Concept of the duty cycle (**a**) with its relation to the mechanical cycle of the motor (**b**).

Duty ratio (r) is the ratio between the attatched time and the total cycle time:

$$r = \frac{\tau_{on}}{\tau_{on} + \tau_{off}} = \frac{\tau_{on}}{\tau_{total}} \tag{13}$$

In vitro sliding velocity (v), which is the velocity with which a motor molecule immobilized on a substrate (e.g., coverglass) propels the corresponding polymer, can be expressed as

$$v = \frac{\delta}{\tau_{on}}, \tag{14}$$

where δ=step size (displacement in a cycle). From this,the on time is obtained as

$$\tau_{on} = \frac{\delta}{v} \tag{15}$$

The total cycle time (τ_{total}) can be expressed as the inverse of the ATPase rate (V):

$$\tau_{total} = \frac{1}{V}, \tag{16}$$

Substituting into equation (1) the new form of the duty ratio is

$$r = \frac{\delta V}{v}. \tag{17}$$

For a processive motor, $r \to 1$, and for a non-processive motor $r \to 0$. A processive motor (e.g., kinesin, DNA-, RNA-polymerase) remains attached during most of the cycle, while a non-processive motor (e.g., myosin) stays mostly in the detached state. A processive motor is able to carry its load by itself. By contrast, in case of a non-processive motor the ensemble of many molecules is required. Furthermore, in the case of large **r** small sliding velocity occurs with high ATPase rate and *vice versa*. The step size varies for different motors. For kinesin it is 8 nm, for myosin II it is 5.5 nm. The force generated by motor proteins under isometric conditions is thought to be ≥ 10 pN.

C. Manipulation of single motor proteins

Single motor proteins are usually investigated by using optical tweezers in various different geometric arrangements. The data analyzed is the position sensor signal from the trapped bead that is linked to the motor protein via the respective polymer molecule. Depending on whether the motor molecule is processive or non-processive, quite different traces are obtained (**Figure 15**) [17]. An unloaded bead captured in the trap displays thermal motion, and the trace corresponds to Brownian noise. A non-processive motor (e.g., myosin) interacts with the filament once in a while, which results in a reduction of the noise. Subsequently, the motor dissociates from the filament and Brownian noise is observed again. A processive motor (e.g., kinesin, DNA and RNA poymerase) holds on to the polymer for an extended period of time. As a result, a progressive shift in the bead position is observed as a function of time (**Figue 15.b**) [19].

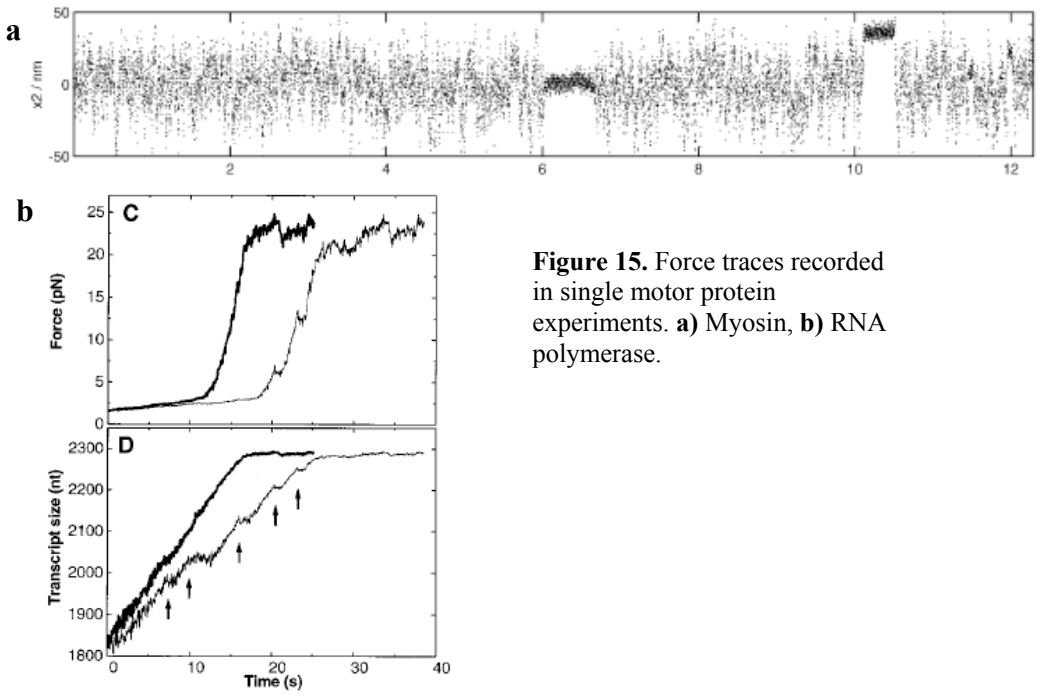

Figure 15. Force traces recorded in single motor protein experiments. **a)** Myosin, **b)** RNA polymerase.

MECHANICS OF SINGLE PROTEIN MOLECULES

In recent years an increasing number of proteins are being directly manipulated with single-molecule methods. Single-molecule techniques provide a unique method to investigate the protein folding problem. The first protein to be mechanically stretched was the giant muscle protein titin [11-13]. Titin is used here as the prototype protein with which the single protein molecule mechanics can be introduced.

A. Prototype protein: the giant muscle protein titin

Titin is a ~3.5-mDa filamentous protein that constitutes about 10% of the total mass of vertebrate muscle proteins [28-31]. This giant molecule spans the half sarcomere, from the Z-line to the M-line (**Figure 16**). Titin is anchored to the Z-line and to the myosin-containing thick filaments of the A-band via its strong myosin-binding property. The I-band segment of the molecule consists of serially-linked tandem immunoglobulin (Ig) domains interrupted with a proline (P)-, glutamate (E)-, valine (V)- and lysine (K)-rich segment (hence named PEVK segment) and other unique sequences [32, 33]. Upon sacomere stretch, passive force is generated by the extension of the I-band segment of titin. The A-band segment of titin on the other hand is composed of super-repeats of Ig and fibronectin (FN) domains. Titin's A-band segment does not participate in the generation of passive force under normal, physiological conditions, but remains attached to the stiff thick filaments. This portion of the molecule is thought to provide a structural scaffold for the thick filament.

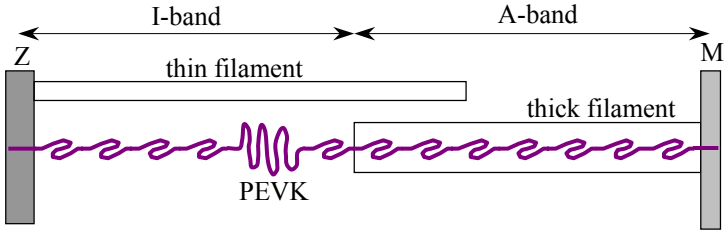

Figure 16. Schematic representation of the structure of the vertebrate muscle half sarcomere. Titin extends form the Z- to the M-line. The globular domains of titin are indicated as simple folds. The PEVK segment is thought to be a highly flexible part of titin, indicated by the spring-like representation. Although titin is shown here as if it runs inside the thick filament, the exact arrangement is not precisely known.

B. Force response of the titin molecule

An extensive review on single titin-molecule mechanics has recently been published [34]. In the raw force vs. extension curve of titin (**Figure 17**), recorded with optical tweezer, force during stretch initially rises nonlinearly (between points A and B). Then titin departs from the initial non-linear elastic behavior, and a force transition begins. This stretch transition (see below) takes place until the maximum experimental force is reached in point C. Upon release, force drops rapidly, and we initially observe a characteristic non-linear force response. Subsequently, a force transition (release transition, see below) begins at point D. Titin can be extended to lengths exceeding the ~1 μm length of the native, folded (but straightened) titin molecule, indicating that part of the extension most likely occurs at the expense of unfolding in the molecule.

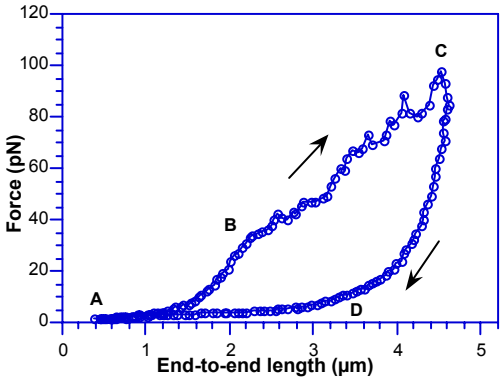

Figure 17. Raw force vs. extension curve obtained for a titin tether. Stretch-release rate, 50 nm/s. Arrows indicate direction of data acquisition (stretch or release). Letters indicate the onset of significant events in the stretch-release cycle (see text).

The non-linear force response can be explained with the entropic polymer nature of titin. Titin's non-linear elastic behavior can be well described with the wormlike chain (WLC) model (**equation 9**). The theoretical WLC curves fit the non-linear portions of the data well both during stretch (**Figure 18.a**) and during release (**Figure 18.b**).

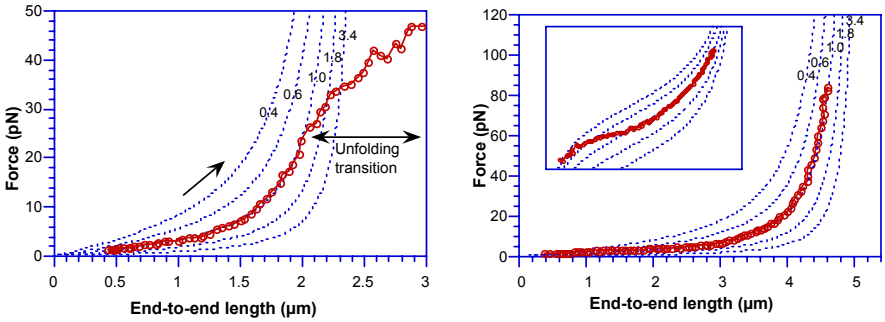

Figure 18. Comparison of the stretch data (**left**) and the release data (**right**) with theoretical wormlike chain (WLC) curves. The dotted lines are WLC curves for chains of different bending rigidities, with their persistence lengths indicated in nanometers. (b, inset) Release data shown on logarithmic force scale. Stretch (unfolding) and release (refolding) force transitions, where the data deviate from WLC behavior, are indicated with arrows.

At high forces during stretch the force curve deviates from the predictions of the WLC model (**Figure 18.a**) because force drops below the theoretical values. The phenomenon can be reconciled with an overstretch of the polymer which results in the increase of its effective contour length. The process is driven by the unfolding of globular domains in titin. Hence, we call the stretch transition unfolding transition. Domain unfolding continues to occur until the maximum experimental force is reached, or as long as folded domains remain in the chain. During release another transition occurs, at low forces (**Figure 18.b**). Here the experimental force increases above the theoretical values, caused by shortening of the effective contour length of the chain, driven by domain refolding. This refolding transition can be particularly well seen when the force is displayed on logarithmic scale (**Figure 18.b. inset**).

Hysteresis, characteristic of non-equilibrium processes, is typical for the force-response of titin. Hysteresis appears because the rate at which we stretch or release titin exceeds the rate of unfolding and refolding at equilibrium at the given extension. Thus, application of the external force displaces the domain folding/unfolding reaction from the

state of equilibrium. If the stretch and release protocols were carried out at considerably slower (infinitely slow) rates, then the stretch and release curves would merge into a single, equilibrium unfolding/refolding force curve. Alternatively, if titin was kept in the unfolded state, hysteresis should disappear, and we should observe an equilibrium force curve. Indeed, the addition of 4 M guanidine-HCl, a chemical denaturant, abolished hysteresis (**Figure 19**). Since the release force curve retraces the stretch curve, the molecule is in a state of conformation equilibrium. Thus, the hysteresis in the experiments was indeed related to the kinetics of domain unfolding and refolding.

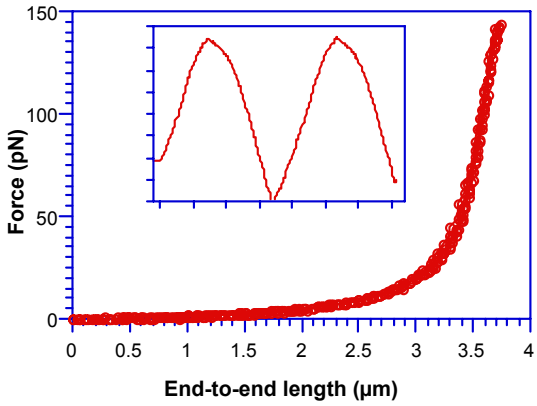

Figure 19. Force vs. extension curve of titin in the presence of 4 M of the chemical denaturant guanidine-HCl. Inset shows the stretch-release protocol as the change in titin's end-to-end length as a function of time. Note that the data were obtained in two consecutive stretch-release cycles. Force hysteresis is completely absent.

C. Stretching titin with the AFM

Titin, and other proteins, can be stretched with the AFM as well. Stretching proteins with the AFM has been pioneered by the groups of Gaub [11] and Fernandez [35]. Titin lends itself naturally to AFM stretching experiments (see **Figure 8**), because it has a modular structure. The distinct modules have been shown to unfold one-by-one in an all-or-none event. Data obtained in an AFM stretching experiment is called force spectrum. The force spectrum of full-length titin obtained in a stretch-release cycle can be seen in **Figure 20**. Titin was stretched by pulling the cantilever rapidly (~1 μm/s) away from the surface. As titin is stretched, force transitions begin to take place (point B) which appear as peaks and valleys (as in a sawtooth) in the force curve. The force transitions correspond to the unfolding of globular domains along the molecule. The domain unfolding process continues until the maximal predetermined length is reached (at point C). During the initial part of release, force drops rapidly in a non-linear fashion (between points C snd D). The non-linear (rising) part of the release force curve

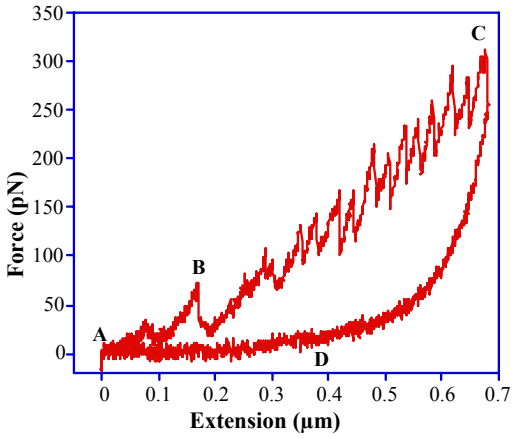

Figure 20. Force spectrum of full-length titin from rabbit longissimus dorsi obtained by using the molecular force probe.

describes a wormlike entropic polymer chain. Once the release half-cycle is complete, the cantilever tip collides with the surface, seen as a sudden drop in force (point A).

The AFM can be used to manipulate recombinant proteins, for example multimodular fragments from the titin sequence (**Figure 21**). By using molecular-biological methods, sequence elements can be replaced and their role in the stability of the protein can be investigated. Such experiments have been used to examine protein isoforms [36], misfolded structures [37], proteins with putative random structures such as the PEVK segment [38], and the structural role of intramolecular hydrogen bonds [39].

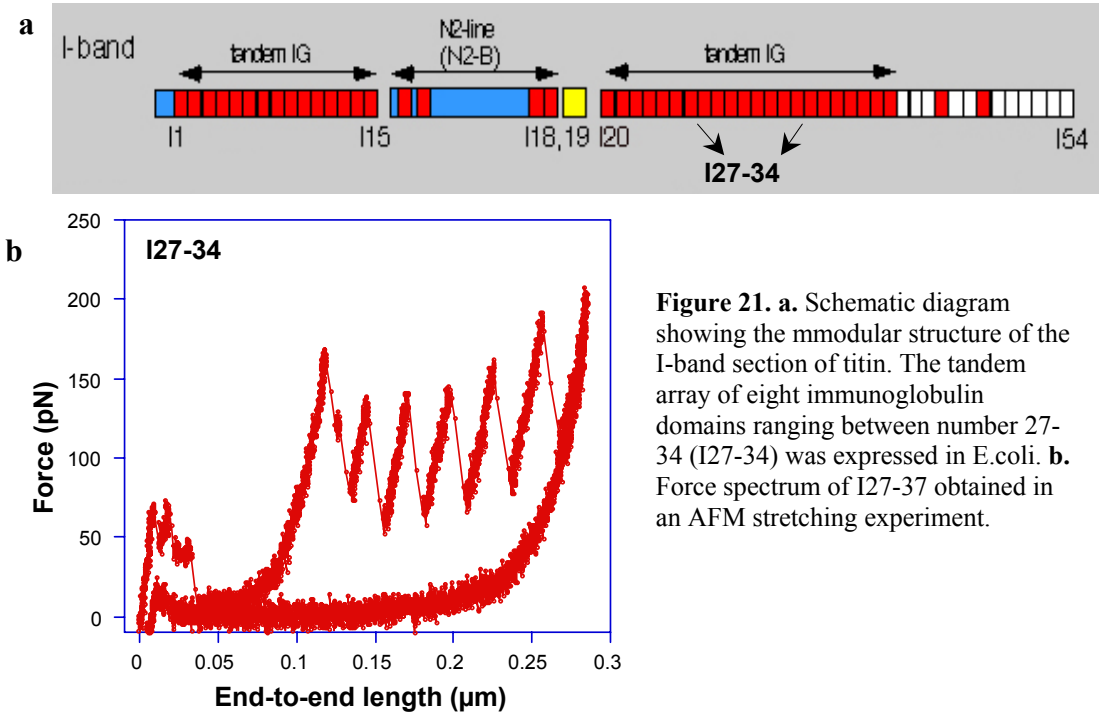

Figure 21. a. Schematic diagram showing the mmodular structure of the I-band section of titin. The tandem array of eight immunoglobulin domains ranging between number 27-34 (I27-34) was expressed in E.coli. **b.** Force spectrum of I27-37 obtained in an AFM stretching experiment.

Sretching modular proteins and protein modules by using the AFM is becoming a common tool in structural biology and protein chemistry .

MECHANICS OF INTERMOLECULAR INTERACTIONS

Single-molecule tools can be used to explore the interaction between molecules. The interaction between various biomolecules has been studied (e.g., streptavidin-biotin, avidin-biotin, antigen-antibody complex) [20, 40-42]. Furthermore, the strength of a covalent bond has also been explored [43]. Intermolecular interactions can be studied by using either optical tweezers (see **Figure 9**) or AFM. When the interaction between molecules are studied, an external load (force) is placed on the bond(s) formed between the molecules. The load is increased as a function of time by pulling the molecules apart, which eventually results in bond rupture. The loading rate (r) can be expressed as

$$r = \frac{f}{t} = Kv_s, \tag{18}$$

where K is stifness (combined stiffness of the probe and the molecular system, Nm^{-1}), and v_s is the stretch rate (ms^{-1}). The bond rupture event is recognized as a sudden drop in force. By the same criterion the method can be extended for use in investigating all kinds of interactions (e.g., intramolecular). Examples of force traces obtained in different molecular systems can be seen in **Figure 22** [7]. The variables experimentally measured are the rupture (or unbinding) force (force at which unbinding occurs when the bond is loaded with a force ramp (**Figure 23.a**) [44]) and the loading rate (obtained from the time-dependent force trace just prior to the unbinding event, considering that the force trace might not be linear throughout).

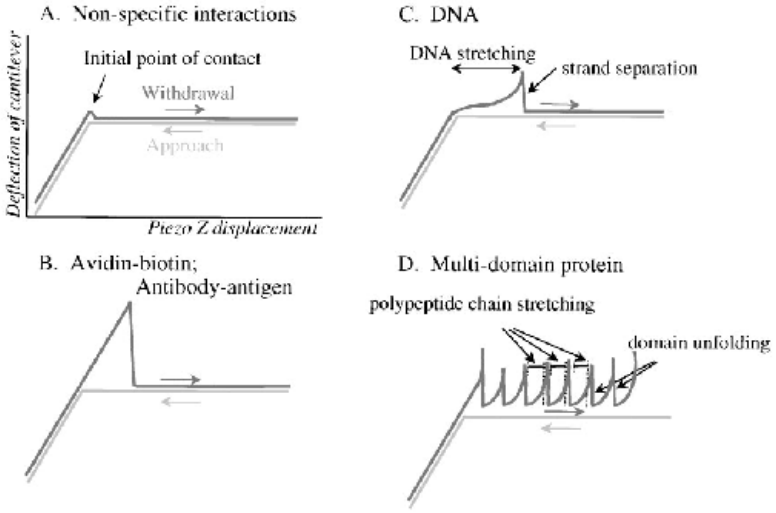

Figure 22. Examples of force traces obtained as a result of different intra- and intermolecular interactions in various biomolecular systems.

The unbinding force is directly related to the unbinding or dissociation kinetics of the molecular complex under load, and therefore depends on the loading rate [45, 46]. In theory it is possible to determine the dissociation rate (hence lifetime) of a bond from the relationship of unbinding force and loading rate. The method has been called dynamic force spectroscopy. The rate of bond dissociation, driven by thermal activation (ν_0), can be expressed as

$$\nu_0 = \omega e^{-\Delta E / k_B T} \tag{19}$$

where, in the context of Kramers' transition state theory, ΔE is the height of the activation energy barrier, $k_B T$ is thermal energy, and ω is an attempt frequency set by Brownian

dynamics (bond vibration frequency). Conceptually, external load tilts the potential energy landscape (**Figure 23.b**) [41, 44], lowers the energy barrier and facilitates bond rupture. The rate of bond rupture under external force (ν_f) can be expressed as

$$\nu_f = \omega e^{-(\Delta E - f\Delta x)/k_B T} = \nu_0 e^{f\Delta x/k_B T}, \qquad (20)$$

where f is the force acting along the reaction coordinate, and Δx is a characteristic distance (along the reaction coordinate) associated with the transition state for bond breaking (width of the energy barrier). Thus, the activation energy barrier is discounted by the mechanical potential (fΔx) and leads to an exponential amplification of the dissociation kinetics.

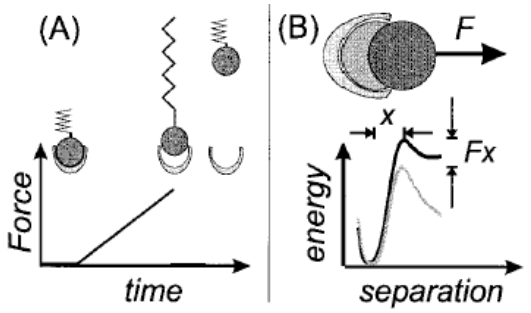

Figure 23. a. Observation of bond rupture under mechanical force. The force on the bond increases until the bond ruptures. **b.** Force-driven dissociation over a sharp activation energy barrier is characterized by a decrease of the barrier with the mechanical potential (Fx).

Bond rupture is a stochastic process, whereby, for a given loading rate (r), a distribution of unbinding forces are observed around a peak unbinding force (f*). For a bond with a single activation energy barrier, f* varies linearly with the natural logarithm of the loading rate , with a slope of $k_BT/\Delta x$, which is expressed as

$$f^* = \frac{k_B T}{\Delta x} \ln \frac{r}{\nu_0 \frac{k_B T}{\Delta x}} \qquad (21)$$

where ν_0 is the thermally activated unbinding rate [44]. Thus, by measuring the slope in the peak unbinding force versus loading rate diagram, one may establish the width of the unbinding potential. In case of multiple linear regimes (**Figure 24**) [41], intermediates of the dissociation may be identified, and the potential energy landscape of the complex (e.g., receptor-ligand) may be constructed.

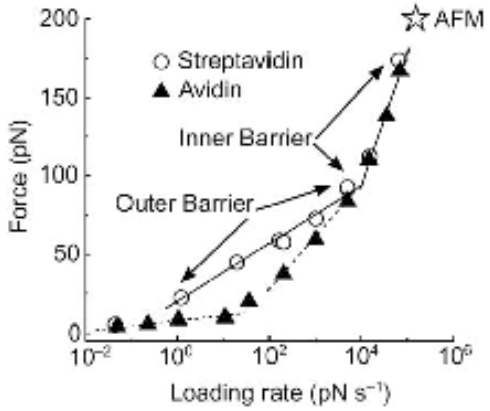

Figure 24. Dynamic strength spectra for biotin streptavidin and biotin-avidin bonds. Based on the different slopes, various activation barriers (and their associated critical distances, Δx) may be identified.

REFERENCES AND SUGGESTED READING

No attempt has been made to provide a comprehensive reference list on the subject. The list below merely scrapes the tip of the iceberg of the single-molecule literature. An emphasis has been placed on citing review papers wherever possible.

1. Bustamante, C., J.C. Macosko, and G.J. Wuite, *Grabbing the cat by the tail: manipulating molecules one by one.* Nat Rev Mol Cell Biol, 2000. **1**(2): p. 130-6.
2. Mehta, A.D., et al., *Single-molecule biomechanics with optical methods.* Science, 1999. **283**(5408): p. 1689-95.
3. Mehta, A.D., M. Rief, and J.A. Spudich, *Biomechanics, one molecule at a time.* J Biol Chem, 1999. **274**(21): p. 14517-20.
4. Strick, T., et al., *Twisting and stretching single DNA molecules.* Prog Biophys Mol Biol, 2000. **74**(1-2): p. 115-40.
5. Svoboda, K. and S.M. Block, *Biological applications of optical forces.* Annu Rev Biophys Biomol Struct, 1994. **23**: p. 247-85.
6. Wang, M.D., *Manipulation of single molecules in biology.* Curr Opin Biotechnol, 1999. **10**(1): p. 81-6.
7. Zlatanova, J., S.M. Lindsay, and S.H. Leuba, *Single molecule force spectroscopy in biology using the atomic force microscope.* Progr Biophys Molec Biol, 2000. **74**: p. 37-61.
8. Smith, S.B., Y. Cui, and C. Bustamante, *Overstretching B-DNA: the elastic response of individual double- stranded and single-stranded DNA molecules.* Science, 1996. **271**(5250): p. 795-9.
9. Cui, Y. and C. Bustamante, *Pulling a single chromatin fiber reveals the forces that maintain its higher-order structure.* Proc Natl Acad Sci U S A, 2000. **97**(1): p. 127-32.
10. Williams, M.C., et al., *Mechanism for nucleic acid chaperone activity of HIV-1 nucleocapsid protein revealed by single molecule stretching.* Proc Natl Acad Sci U S A, 2001. **98**(11): p. 6121-6.
11. Rief, M., et al., *Reversible unfolding of individual titin immunoglobulin domains by AFM.* Science, 1997. **276**(5315): p. 1109-12.
12. Kellermayer, M.S., et al., *Folding-unfolding transitions in single titin molecules characterized with laser tweezers.* Science, 1997. **276**(5315): p. 1112-6.
13. Tskhovrebova, L., et al., *Elasticity and unfolding of single molecules of the giant muscle protein titin.* Nature, 1997. **387**(6630): p. 308-12.
14. Rief, M., et al., *The mechanical stability of immunoglobulin and fibronectin III domains in the muscle protein titin measured by atomic force microscopy.* Biophys J, 1998. **75**(6): p. 3008-14.
15. Baumgartner, W., et al., *Cadherin interaction probed by atomic force microscopy.* Proc Natl Acad Sci USA, 2000. **97**(8): p. 4005-4010.
16. Kellermayer, M.S., et al., *Mechanical manipulation of single titin molecules with laser tweezers.* Adv Exp Med Biol, 2000. **481**: p. 111-26.
17. Knight, A.E., et al., *Analysis of single-molecule mechanical recordings: application to acto- myosin interactions.* Prog Biophys Mol Biol, 2001. **77**(1): p. 45-72.

18. Finer, J.T., R.M. Simmons, and J.A. Spudich, *Single myosin molecule mechanics: piconewton forces and nanometre steps.* Nature, 1994. **368**(6467): p. 113-9.
19. Wang, M.D., et al., *Force and velocity measured for single molecules of RNA polymerase.* Science, 1998. **282**: p. 902-907.
20. Stout, A.L., *Detection and characterization of individual intermolecular bonds using optical tweezers.* Biophys J, 2001. **80**(6): p. 2976-86.
21. Bustamante, C., et al., *Single-molecule studies of DNA mechanics.* Curr Opin Struct Biol, 2000. **10**(3): p. 279-85.
22. Marko, J.F. and E.D. Siggia, *Stretching DNA.* Macromolecules, 1995. **28**: p. 8759-8770.
23. Houchmandzadeh, B. and S. Dimitrov, *Elasticity measurements show the existence of thin rigid cores inside mitotic chromosomes.* J Cell Biol, 1999. **145**(2): p. 215-23.
24. Liphardt, J., et al., *Reversible unfolding of single RNA molecules by mechanical force.* Science, 2001. **292**(5517): p. 733-7.
25. Zhuang, X., et al., *A single-molecule study of RNA catalysis and folding.* Science, 2000. **288**(5473): p. 2048-51.
26. Howard, J., *Mechanics of Motor Proteins and the Cytoskeleton*. 2001, Sunderland, MA: Sinauer Associated, Inc.
27. Howard, J., *Molecular motors: structural adaptations to cellular functions.* Nature, 1997. **389**(6651): p. 561-7.
28. Gregorio, C.C., et al., *Muscle assembly: a titanic achievement?* Curr Opin Cell Biol, 1999. **11**(1): p. 18-25.
29. Maruyama, K., *Connectin/titin, giant elastic protein of muscle.* Faseb J, 1997. **11**(5): p. 341-5.
30. Trinick, J. and L. Tskhovrebova, *Titin: a molecular control freak.* Trends Cell Biol, 1999. **9**(10): p. 377-80.
31. Wang, K., *Titin/connectin and nebulin: giant protein rulers of muscle structure and function.* Adv Biophys, 1996. **33**: p. 123-34.
32. Freiburg, A., et al., *Series of exon-skipping events in the elastic spring region of titin as the structural basis for myofibrillar elastic diversity.* Circ Res, 2000. **86**(11): p. 1114-21.
33. Labeit, S. and B. Kolmerer, *Titins: giant proteins in charge of muscle ultrastructure and elasticity.* Science, 1995. **270**(5234): p. 293-6.
34. Wang, K., J.G. Forbes, and A.J. Jin, *Single molecule measurements of titin elasticity.* Prog Biophys Mol Biol, 2001. **77**(1): p. 1-44.
35. Fisher, T.E., et al., *The study of protein mechanics with the atomic force microscope.* Trends Biochem Sci, 1999. **24**(10): p. 379-84.
36. Carrion-Vazquez, M., et al., *Atomic force microscopy captures length phenotypes in single proteins.* Proc Natl Acad Sci U S A, 1999. **96**(20): p. 11288-92.
37. Oberhauser, A.F., et al., *Single protein misfolding events captured by atomic force microscopy.* Nature Struct Biol, 1999. **6**: p. 1025-1028.
38. Li, H., et al., *Multiple conformations of PEVK proteins detected by single-molecule techniques.* Proc Natl Acad Sci U S A, 2001. **98**(19): p. 10682-6.
39. Marszalek, P.E., et al., *Mechanical unfolding intermediates in titin modules.* Nature, 1999. **402**(6757): p. 100-3.

40. Dammer, U., et al., *Specific antigen/antibody interactions measured by force microscopy.* Biophys J, 1996. **70**(5): p. 2437-41.
41. Merkel, R., et al., *Energy landscapes of receptor-ligand bonds explored with dynamic force spectroscopy.* Nature, 1999. **397**(6714): p. 50-3.
42. Yuan, C., et al., *Energy landscape of streptavidin-biotin complexes measured by atomic force microscopy.* Biochemistry, 2000. **39**(33): p. 10219-23.
43. Grandbois, M., et al., *How strong is a covalent bond?* Science, 1999. **283**(5408): p. 1727-30.
44. Strunz, T., et al., *Model energy landscapes and the force-induced dissociation of ligand- receptor bonds.* Biophys J, 2000. **79**(3): p. 1206-12.
45. Bell, G.I., *Models for the specific adhesion of cells to cells.* Science, 1978. **200**(4342): p. 618-27.
46. Evans, E. and K. Ritchie, *Dynamic strength of molecular adhesion bonds.* Biophys J, 1997. **72**(4): p. 1541-55.